RESEARCH ARTICLE

Sequestosome-1 (p62) expression reveals chaperone-assisted selective autophagy in immune-mediated necrotizing myopathies

Norina Fischer[1,*]; Corinna Preuße[1,*]; Josefine Radke[1]; Debora Pehl[2]; Yves Allenbach[3]; Udo Schneider[4]; Eugen Feist[4]; Vincent von Casteleyn[4]; Katrin Hahn[5]; Tobias Ruck[6]; Sven G. Meuth[6]; Hans-Hilmar Goebel[1]; Rose Graf[7]; Andrew Mammen[7]; Olivier Benveniste[3]; Werner Stenzel[1,8] (iD)

[1] Department of Neuropathology, Charité - Universitätsmedizin, Freie Universität Berlin, Humboldt-Universität zu Berlin, and Berlin Institute of Health (BIH), Berlin, Germany.

[2] Oxford University Hospitals Foundation Trust, Neuropathology & Ocular Pathology Department, John Radcliffe Hospital, Oxford, OX3 9DU, UK.

[3] Assistance Public-Hôpitaux de Paris, Sorbonne-Université, INSERM, UMR974, Department of Internal Medicine and Clinical Immunology, Pitié-Salpêtrière University Hospital, Paris, France.

[4] Department of Rheumatology, Charité - Universitätsmedizin, Freie Universität Berlin, Humboldt-Universität zu Berlin, and Berlin Institute of Health (BIH), Berlin, Germany.

[5] Department of Neurology, Charité - Universitätsmedizin, Freie Universität Berlin, Humboldt-Universität zu Berlin, and Berlin Institute of Health (BIH), Berlin, Germany.

[6] Department of Neurology with Institute for Translational Neurology, University Hospital Münster, Münster, Germany.

[7] National Institutes of Health, 9000 Rockville Pike, Building 50, Room 1505, Bethesda, MD 20892, USA.

[8] Leibniz ScienceCampus Chronic Inflammation, Berlin, Germany.

Abstract

Diffuse myofiber necrosis in the context of inflammatory myopathy is the hallmark of immune-mediated necrotizing myopathy (IMNM). We have previously shown that skeletal muscle fibers of IMNM patients may display nonrimmed vacuoles and sarcoplasmic irregularities. The dysfunctional chaperone activity has been linked to the defective assembly of skeletal muscle proteins and their degradation via lysosomes, autophagy and the proteasomal machinery. This study was undertaken to highlight a chaperone-assisted selective autophagy (CASA) pathway, functionally involved in protein homeostasis, cell stress and the immune response in skeletal muscle of IMNM patients. Skeletal muscle biopsies from 54 IMNM patients were analyzed by immunostaining, as well as by *q*PCR. Eight biopsies of sIBM patients served as pathological controls, and eight biopsies of nondisease control subjects were included. Alteration of autophagy was detectable in all IMNM biopsy samples highlighted via a diffuse sarcoplasmic staining pattern by p62 and LC3 independent of vacuoles. This pattern was at variance with the coarse focal staining pattern mostly confined to rimmed vacuoles in sIBM. Colocalization of p62 with the chaperone proteins HSP70 and αB-crystalline points to the specific targeting of misfolded proteins to the CASA machinery. Bcl2-associated athanogene 3 (BAG3) positivity of these fibers emphasizes the selectivity of autophagy processes and these fibers also express MHC class I sarcolemma. Expression of genes involved in autophagy and endoplasmic reticulum (ER) stress pathways studied here is significantly upregulated in IMNM. We highlight that vacuoles without sarcolemmal features may arise in IMNM muscle biopsies, and they must not be confounded with sIBM-specific vacuoles. Further, we show the activation of selective autophagy and emphasize the role of chaperones in this context. CASA occurs in IMNM muscle, and specific molecular pathways of autophagy differ from the ones in sIBM, with p62 as a unique identifier of this process.

Abbreviations: BAG3, Bcl2-associated athanogene 3; CASA, chaperone-assisted selective autophagy; CHIP, C-terminus of HSC70-interacting protein; CK, creatine kinase; DMD, Duchenne muscular dystrophy; ER, endoplasmic reticulum; hIBM, hereditary inclusion body myopathy; HPF, high-power fields; HSC70, heat shock cognate 70; HSPA8, heat shock protein family A (Hsp70) member 8; HSPB8, heat shock protein family B, member 8; HSP70, heat shock protein 70; HMGCR, 3-hydroxy-3-methyl-glutaryl-coenzyme A reductase; IIM, idiopathic inflammatory myopathy; IMNM, immune-mediated necrotizing myopathy; LAMP2, lysosomal-associated membrane protein 2; LC3, microtubule-associated protein 1A/1B light chain; MAAs, myositis-associated autoantibodies; MHC, major histocompatibility complex; MSAs, myositis-specific autoantibodies; NDC, nondisease controls; p62, sequestosome 1; PM, polymyositis; SD, standard deviation; sIBM, sporadic inclusion body myositis; SRP, signal recognition particle; UPR, unfolded protein response; UPS, ubiquitin-proteasome system.

INTRODUCTION

Immune-mediated necrotizing myopathy (IMNM) constitutes a distinct entity among the idiopathic inflammatory myopathies (IIMs) (2) and is paradigmatically linked to anti-SRP and anti-HMGCR, two autoantibodies localized in the endoplasmic reticulum (ER), and detectable in the sera of myositis patients (3). We have recently achieved international consensus on clinical, morphological and serological characteristics of IMNM patients (3). Morphologically, IMNM is characterized by diffusely distributed necrotic myofibers at different stages, numerous regenerating fibers, variable MHC class I expression of the sarcolemma, complement deposition on the sarcolemma and a pauci-lymphocytic infiltrate (3). However, additional features are needed to characterize this entity and differentiate it from other IIMs, offering valuable insights into pathomechanisms of IMNM as well. More specifically, these comprise nonrimmed vacuoles and sarcoplasmic irregularities, which we have further addressed in this paper. Both features may arise in a variety of neuromuscular diseases ranging from childhood or adult-onset hereditary ones to sporadic inclusion body myositis (sIBM) or drug-induced myopathies. In sIBM, vacuoles are considered to be a part of the obligatory morphologic diagnostic criteria, though their imperative presence has been questioned (26). A thorough analysis of several diagnostic molecules has identified p62 staining as the most reliable histological tool for sIBM (14). Additionally, several key molecules linked to autophagy have been highlighted in sIBM and hereditary inclusion body myopathy (hIBM) recently (20, 44), and are presumably involved in the pathogenesis of sIBM.

Macroautophagy, the classical form of autophagy as opposed to microautophagy, involves the *de novo* formation of autophagolysosomes (9). Chaperone-assisted selective autophagy (CASA) was characterized by starvin [Bcl2-associated athanogene 3 (BAG3) homologue]-deficient drosophila (6), and is characterized by the interaction of the chaperone complex, consisting of BAG3/CHIP/HspB8/Hsp70, with p62. The ubiquitin ligase CHIP, interacting with the chaperones Hsp70 and Hsp90 and being a supplier of the ubiquitin-proteasome system (UPS) with degradation prone substrates (6), recognizes and facilitates ubiquitylation of BAG3/Hsc70/HspB8-held proteins (5). Consecutively, BAG3/CHIP recruits p62, which acts as a connecting element between the CASA complexes plus its ubiquitylated protein and the formation of autophagosome. BAG3 and p62 are ubiquitylated by themselves and therefore efficiently recycled with the autophagosome contents (13, 18). We have focused on these molecules since we hypothesized that they may be involved in autophagolysosomal pathways in IMNM.

BAG3 mutations may also lead to severe myofibrillar myopathy (41), cardiomyopathy (35) and neuropathy (36), highlighting the relevance of this molecule in the neuromuscular system.

Moreover, we have recently highlighted that the lysosome-independent immune proteasome machinery is involved in the degradation of antigen peptides presented at the cellular surface via MHC class I in IMNM (12). Finally,

ER stress and the unfolded protein response (UPR), pathways that deal with the processing of proteins transported to the ER, comprising a multitude of different regulating chaperones, may also be altered in certain forms of myositis.

This work addresses the abovementioned pathways and their putative interaction and pathophysiological implications in IMNM.

MATERIAL AND METHODS

Patient cohort

Clinical data of 54 IMNM patients, eight sIBM patients and eight control patients lacking any clinical, laboratory or pathomorphological findings enrolled in this study are listed in Table 1. We included patients with typical clinical, serological and morphological signs and symptoms of IMNM (3). Informed consent was obtained from all patients at each institution involved. All procedures were approved by the official ethical standards committee (EA2/163/17) at the Charité - Universitätsmedizin Berlin, Germany.

Skeletal muscle specimen

We analyzed skeletal muscle biopsies from 54 patients diagnosed with IMNM according to the clinico-sero-morphological European Neuromuscular Centre (ENMC) criteria (3). Also, skeletal muscle biopsies from eight sIBM patients were included (clinical and morphological definitive sIBM) (39). Furthermore, we investigated control skeletal muscle biopsies (n = 8) from patients with nonspecific muscle/soft tissue complaints, for whom muscle weakness (clinically)

Table 1. Clinical data of IMNM patients, sIBM pathological controls and nondisease controls (NDC).

	IMNM	sIBM	NDC
	n = 54	n = 8	n = 8
With vacuoles	81% (44)	100% (8)	
w/o vacuoles	19% (10)		100% (8)
Age	56.7 ± 18	72.9 ± 4	22.3 ± 19
Sex			
Female	65% (35)	25% (2)	50% (4)
Male	35% (19)	75% (6)	50% (4)
Antibodies			
SRP	41% (23)		
HMGCR	32% (16)		
Unknown	27% (15)		
Not measured		100% (8)	100% (8)
Duration of symptoms			
<3 years	52% (28)	13% (1)	100% (8)
>3 years	17% (9)	50% (4)	
Unknown	34% (19)	38% (3)	
CK			
<10x	15% (8)	75% (6)	100% (8)
>10x	80% (43)		
Unknown	5% (3)	25% (2)	

and morphological abnormalities on skeletal muscle biopsy were excluded. Their CK levels were normal; no signs of systemic inflammation and no myositis-specific (MSAs) or myositis-associated autoantibodies (MAAs) were detected. The muscle specimens were cryopreserved at -80°C for the routine diagnostic workup and a part was preserved in glutaraldehyde for the ultrastructural analysis.

Histologic, enzyme histochemical, immunohistochemical and immunofluorescence procedures

Routine stains were performed in 7 µm cryostat sections, according to standard procedures. Immunohistochemical and double immunofluorescence stains were obtained as described previously (37). The following antibodies were used for staining procedures: (Primary antibody, Dilution; Company/ Clone): αB-crystallin, dil. 1:2500; Abcam/1B6.1-3G4, BAG3, dil. 1:500; Abcam/polyclonal, ß amyloid, dil. 1:3000; Covance/4G8, ß Spectrin, dil. 1:100; Novocastra/RBC2/3D5, Caveolin 3, dil. 1:200; BD/26, Dysferlin, dil. 1:5000, Novocastra/HAM1/7B6, Dystrophin 1, dil. 1:10; Novocastra/ Dy4/6D3, FUS, dil. 1:500; Sigma/polyclonal, Hsp70, dil. 1:100; Abcam/ab6535, LAMP-2, dil. 1:500; Santa Cruz/5H2, LC3, dil. 1:50; Nanotools Art/LC3-2G6, MHC-I, dil. 1:1000; Dako/w6/32, pαSyn, dil. 1:500; WAKO 01525191, Prion protein, dil. 1:500; Covance 3F4, SQSTM1/p62, dil. 1:100, Abcam/rabbit polyclonal 91526, Monoclonal mouse α-human p62, dil. 1:100; RD transduction lab 3/p62, Tau, dil.1:40, Thermo scientific/AT8, TDP43, dil. 1:250; Protein Tech Group/polyclonal.

For further evaluation, cell counts of myofibers positive for p62 or LC3 per 10 high power fields (HPF, one high-power field measures 0.16 mm^2) were conducted. Additionally, a semiquantitative score for the upregulation of MHC class I deposition was applied, with 0 = no sarcolemmal staining; 1 = focal sarcolemmal staining (<30% of myofibers); 2 = 30%–60% of myofibers with sarcolemmal staining (and/ or focal accumulation); 3 = 60% of myofibers with sarcolemmal staining.

Transmission electron microscopy (TEM)

The ultrastructural analysis was performed after the fixation of the muscle specimens in 2.5% glutaraldehyde for 48 hours at 4°C, postfixation in 1% osmium tetroxide, and sample embedding in Araldite. Semi-thin sections were used to identify vacuoles and respective ultrathin sections were stained with uranyl acetate and lead citrate. The EM 902 electron microscope (Zeiss, Oberkochen, Germany) was used to analyze the specimens.

Quantitative reverse transcription PCR (qRT-PCR)

Total RNA was extracted from muscle specimens using the technique described previously by our group (37). Afterward cDNA was synthesized using the High-Capacity cDNA

Archive Kit (Applied Biosystems, Foster City, CA). For qPCR reactions, 2 ng of cDNA was used, and for the analysis, the 7900HT Fast Real-Time PCR System (Applied Biosystems, Foster City, CA) was used and running conditions were 95 °C 0:20, 95 °C 0:01 and 60 °C 0:20, for 45 cycles (values above 40 cycles were defined as not expressed). All genes were run as triplicates and each run contained the reference gene (PGK1) as internal control, to normalize the expression of the target genes. The qPCR assay identification numbers, TaqMan® Gene Expression Assay from Life Technologies/Thermo Fisher are listed as follows: *HSPB5 (CRYAB)* Hs00157107_m1; *BECN1* Hs00186838_m1; *LC3 (MAP1LC3A)* Hs01076567_g1; *p62 (SQSTM1)* Hs02621445_ s1; *ULK1/ATG1* Hs00177504_m1; *BAG3* HS00188713_m1; *XBP1* Hs00231936_m1; *EDEM1* Hs00976004_m1; *HSPA5/ GRP78* Hs00607129_gH; *HSPA8* Hs03044880_gH; *HSPB8* Hs00205056_m1; *DDIT3/CHOP*, Hs00358796_g1; *PGK1* Hs99999906_m1.

The ΔCT of "normal" controls was subtracted from the ΔCT of IMNM patients to determine the differences (ΔΔCT) and fold change ($2^{\wedge}$-ΔΔCT) of gene expression. Gene expression was illustrated by the log10 of fold change values compared to nondisease controls (NDC).

Statistical analysis

Kruskal-Wallis one-way ANOVA followed by the Bonferroni-Dunn correction of the *post hoc* tests was used to analyze the quantitative differences of mRNA transcripts. Data are presented as mean ± SEM. The level of significance was set at $P < 0.05$. The GraphPad Prism 5.02 and 7.01 software (GraphPad Software, Inc., La Jolla, CA, USA) was used for statistical analysis.

RESULTS

Clinical data

Clinical parameters of 54 IMNM patients were included in the retrospective clinical analysis of the study. Females were 65% (35 patients). The mean age at the time of biopsy was 56.7 years (standard deviation (SD) of ± 18.1), with the youngest patient being 16 and the oldest being 92 years at the time of biopsy. Female patients were 54.4 years old on an average, whereas male patients showed an average age of 61 years (no significant difference). All patients suffered from proximal tetraparesis, which was more pronounced in the lower limbs (see Table 1). The duration of disease at the time of biopsy was 26 months on an average (SD of ± 41.6).

Anti-SRP-autoantibodies were harbored by 41% (23 patients) of all patients, 32% (16 patients) had anti-HMGCR-autoantibodies and for 27% (15 cases) the autoantibody status was unknown and not obtainable retroactively. A highly increased CK value (>10-fold) was observed in 80% of patients, while the remaining patients had moderately increased values (up to 10-fold).

Autophagolysosomal pathways are activated in IMNM

The IMNM patient biopsies were grouped and analyzed separately according to the presence or absence of vacuoles (V+ 81%, V− 19%). Compared to NDC, V+ IMNM skeletal muscle biopsies showed significantly increased levels of *LC3* gene expression, encoding for a protein (LC3I) that marks autophagosomal structures from the forming phagophore until fusion with lysosomes. The same is true in sIBM cases, while there is no significant difference between IMNM and sIBM (Figure 1A). *SQSTM1* encoding for p62, a protein that connects polyubiquitinylated proteins with LC3, is not differentially regulated in IMNM skeletal muscle biopsies or in sIBM compared to NDC. There was no significant increase of *BECLIN* or *ULK1*, both genes related to the initiation of autophagy, in the IMNM groups or compared to NDC (Figure 1A). However, *ULK1* expression in sIBM patients was significantly reduced as compared to NDC, as well as to either IMNM group. There was no difference between anti-SRP and anti-HMGCR specimens or those without known antibody status and there was no significant difference in SRP or HMGCR frequency in the 18% of biopsies without vacuoles (data not shown).

Though we did not identify any significant difference in the gene expression of *p62* or *LC3* when comparing the V+ and V− IMNM groups, we did see significantly more p62+ and LC3+ myofibers in biopsies harboring vacuoles (V+) as compared to biopsies without vacuoles (V−) even though this did not reach statistical significance. Only p62 in V− reached significance (adjusted *p*-value 0.0092 when compared to sIBM (Figure 1C). Interestingly, V+ biopsies had generally more necrotic myofibers, suggesting that necrosis and myophagocytosis may be linked to vacuole formation rather than macroautophagic processes (adjusted p-value V− vs. V+ 0.0759; Figure 1B,C). Indeed, numbers of

macrophages and fibers exhibiting myophagocytosis were significantly more important in V+ as compared to V− biopsies of IMNM patients (*P* < 0.05), and still sIBM patients had even higher numbers of fibers with myophagocytosis (*P* < 0.05) compared to V+ biopsies (data not shown).

Histological staining of p62 and LC3 (antibody recognizes both LC3I and -II) revealed a uniform pattern in all skeletal muscle specimens from IMNM patients irrespective of anti-SRP or anti-HMGCR positivity in patients' sera, with a diffusely fine and homogenous sarcoplasmic staining in a variable amount of muscle fibers, whereas NDC specimens consistently showed no overt staining of their sarcoplasm (Figure 2A,B,D, and Figures S1 and S2). LC3+ and p62+ fibers were not necrotic or regenerating and did not show myophagocytosis, and both stains were not specifically clustering in or around vacuoles. This pattern was obtained identically by both a monoclonal anti-mouse antibody and a polyclonal anti-rabbit antibody (see methods). In contrast, staining of p62 or LC3 in sIBM patients appeared as focal sarcoplasmic strongly stained (dark) deposits mostly in vacuoles, close to the sarcolemma or surrounding the nucleus (Figure 2C,F). We did not observe any punctate p62 staining in toxic myopathies and in genetic myopathies/dystrophies (dysferlinopathy, anoctaminopathy, FSHD, etc.) with necrotic myofibers (data not shown). Staining of lysosomes as displayed by LAMP2 immunohistochemistry was strong both in V+ and in V− IMNM also with a diffuse character, and sIBM showed a similar pattern for LAMP immunohistochemistry (Figure 2G–I).

Prominent increase of autophagy in IMNM skeletal muscle specimen is not confined to vacuoles

Further, specific analysis of vacuoles in skeletal muscle biopsies from patients with IMNM revealed that 81% had vacuoles irrespective of the associated autoantibody in the
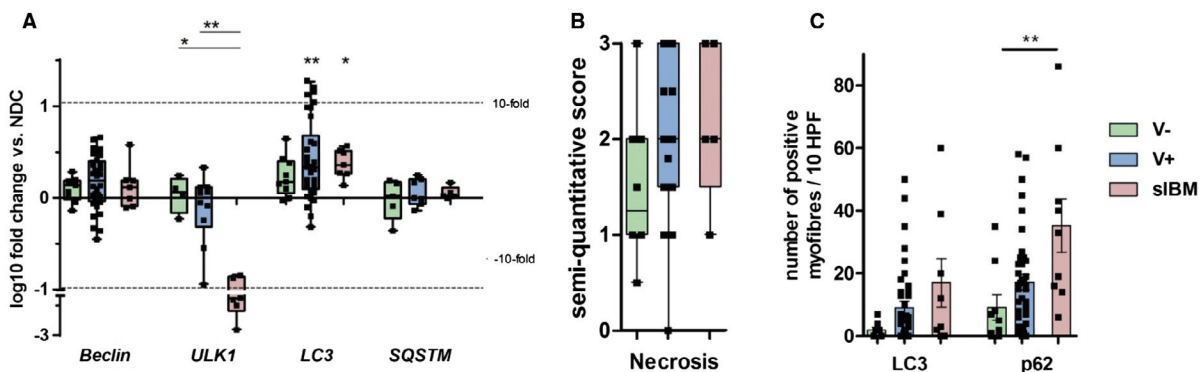
Figure 1. *Gene expression levels of autophagy-related genes in IMNM and sIBM.* **A.** mRNA levels of autophagy-related gene *LC3* were significantly increased in V+ patients compared to NDC, while *p62*, *Beclin* and *ULK1* levels were not in either IMNM groups, while sIBM patients had significantly reduced expression of *ULK1*. **B.** Semi-quantitative score of necrosis and myophagocytosis in IMNM biopsies with (V+) and without (V−) vacuoles, assessed by stains for nonspecific esterase and H&E showed a higher number of necrosis and myophagocytosis in the vacuole positive (V+) group when compared to

the vacuole negative (V−) group, while sIBM patients showed a constantly high value of 3. **C.** Histomorphological evaluation revealed similar numbers of LC3 positive fibers in the V+ and V− group, while V+ patients showed a significantly higher number of myofibers staining with p62, without any statistical significance. However, V− reached significance when compared to sIBM (adjusted *p*-value 0.0092). Statistical analysis was performed using Kruskal-Wallis one-way ANOVA with Dunn's multiple comparison test. (*P* < 0.05, **P* < 0.001 and ***P* < 0.0001).
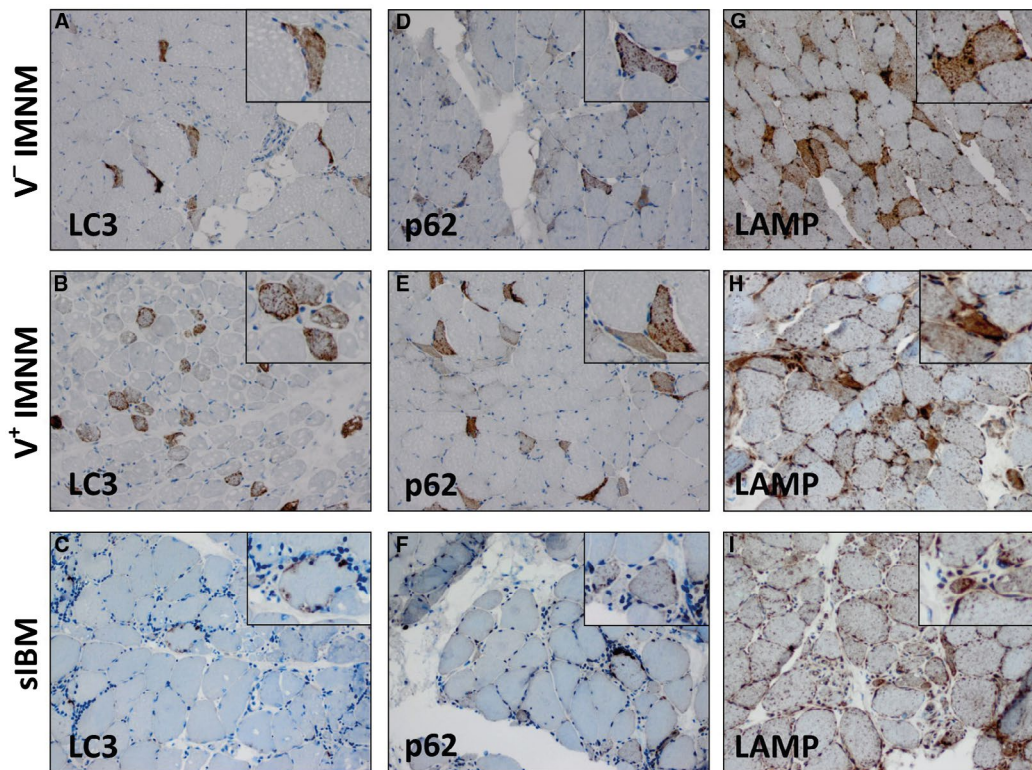
Figure 2. *Staining pattern of p62, LC3 and LAMP2 in IMNM and sIBM.* LC3 (A, B) and p62 (D, E) stains in IMNM skeletal muscle biopsies show a fine granular pattern throughout the entire sarcoplasm with variable intensity. Numbers of p62- or LC3-positive fibers are higher in the V−IMNM patient biopsies. In the sIBM patient biopsies, the respective autophagy markers show a focal dense staining pattern, which is confined to vacuoles (C, F), for example, in the subsarcolemmal region (C, F inset). Note the absence of staining in/around a vacuole in E (inset). LAMP2-positive diffuse sarcoplasmic stains (G, H) with different intensity staining lysosomes and mirroring the autophagy pattern displayed by p62 and LC3, while in sIBM, the focal accumulation of lysosomes can be noted and diffuse sarcoplasmic staining is consistently absent (I).

sera of IMNM patients (see Table 1). Given that p62 and LC3 stains are well-established methods to highlight vacuoles in sIBM (14, 34, 39), we were intrigued by the fact that we did not see any p62+ or LC3+ vacuoles in IMNM biopsies. Vacuoles were not rimmed and did not exhibit any sarcolemmal features, as they were not lined by sarcolemmal proteins (dystrophin-1, dysferlin, caveolin-3 and β-spectrin) (not shown). None of them contained any of the following proteins: tau protein, prion protein, beta-amyloid, FUS, TDP-43 and pα synuclein. They were not birefringent by Congo red staining and were thioflavin-negative (not shown).

CASA is specifically altered in IMNM biopsies

The intriguing homogenous and finely dotted sarcoplasmic p62 or LC3 staining patterns constantly present in IMNM biopsy samples led us to hypothesize that molecules involved in protein turnover may be involved in the observed enhanced autophagy pathways. We, therefore, investigated BAG3, HSP70 and αB-crystallin molecules crucially involved in the CASA pathway. P62 positive fibers were identical to those

stained by HSP70, αB-crystallin (HSPB5) and BAG3, which is highlighted by serial sections (Figure 3A–D), and double immunohistochemistry of p62 with BAG3, p62 with αB-crystallin and p62 with HSP70 verified this feature (Figure 3E–G). Interestingly, there was no significant upregulation of these markers on the mRNA level, as shown by the measurement of mRNA transcripts in IMNM patients (Figure 3H). The same was true for *BAG3*, which was not altered in IMNM, but interestingly it significantly reduced in sIBM biopsies compared to V+ (Figure 3H). Conversely, αB-crystallin did not significantly colocalize with p62 in sIBM, and HSP70 was also not found in vacuolar structures (Figure S3), but stained occasional fibers heterogeneously. In addition, mRNA levels of *HSPA5/GRP78* in IMNM, encoding for a constitutive ER chaperone protein that binds ER-stress sensing molecules in their inactivated state, were expressed to a similar degree (not significantly elevated) as compared to control biopsies (data not shown). Taken together, key molecules involved in CASA are obviously altered in the protein level and RNA level as well as shown by TEM in IMNM pathophysiology.
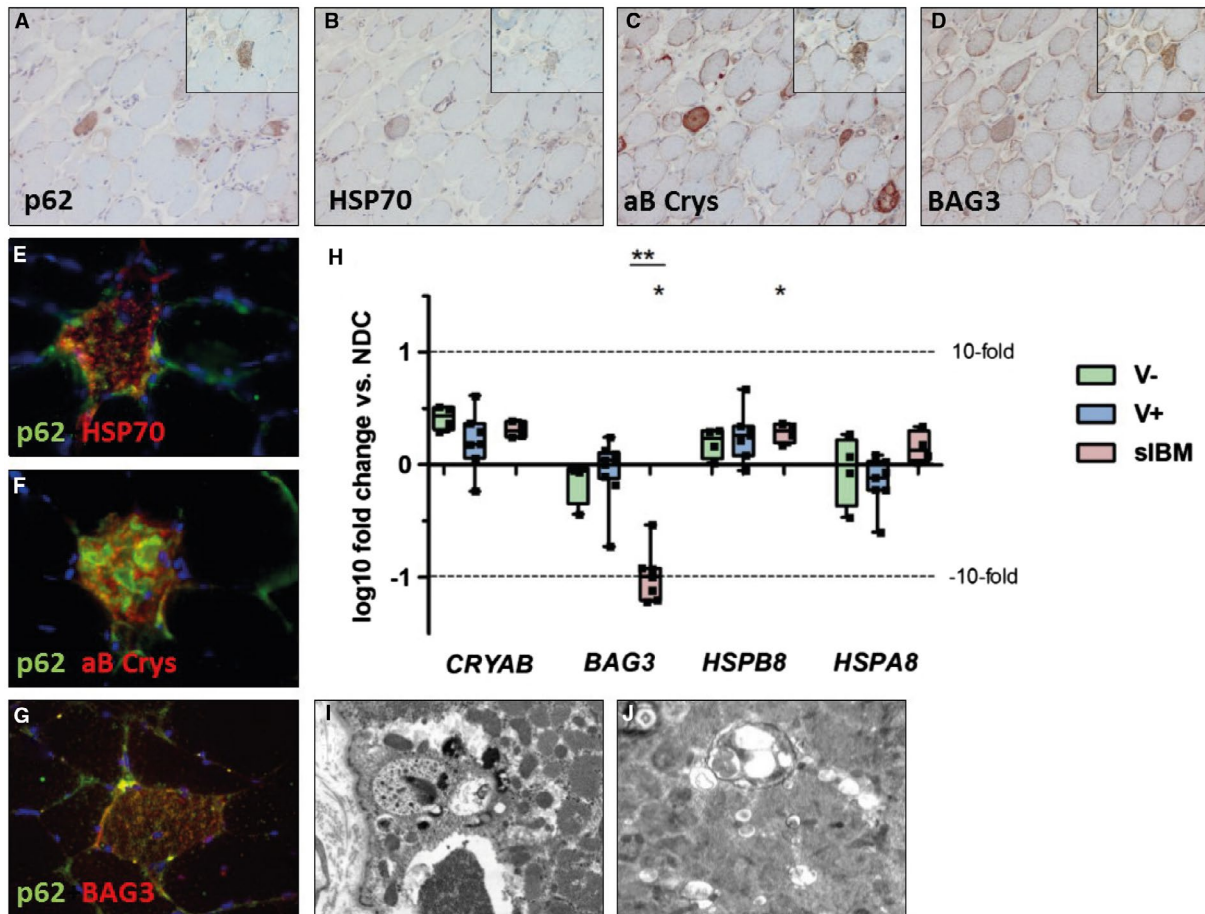
Figure 3. *Gene expression and staining pattern of CASA-related molecules in IMNM and sIBM.* Serial muscle sections demonstrate the staining of various chaperone-assisted selective autophagy (CASA) markers in the same skeletal muscle fiber. A p62 (**A**) positive fiber also stains positive for HSP70 (**B**), αB-crystallin (**C**) and BAG3 (**D**); original magnification x200. **E-G.** double immune fluorescence demonstrates the staining of p62 and HSP70, αB-crystallin and BAG3 in the same fiber; original magnification x1000. **H.** Gene expression levels of these markers show no change of expression of the genes between the IMNM subgroups; however, *BAG3* expression levels are significantly reduced in sIBM patients when compared to V+ IMNM and NDC. In addition, there is a significantly increased expression of *HSPB8* in sIBM when compared to NDC. Magnification of A,B,C and D 200x, Statistical analysis was performed using Kruskal-Wallis one-way ANOVA with Dunn's multiple comparison test. **I,J**: Electron microscopy of vacuoles with various diameters and diffuse distribution (**J**) showing debris and nonspecific granular material in lysosomes; original magifications 10.000-fold. Note absence of any tubular filamentous material (as in sIBM). (*$P < 0.05$, **$P < 0.001$ and ***$P < 0.0001$).

MHC class I upregulation in/on p62+ myofibers

We next questioned how the immune system may recognize "CASA-tagged" myofibers. Since we had previously shown that MHC class I is upregulated on the sarcolemmal surface (in addition to sarcoplasmic positivity) of IMNM myofibers, and that it confers parts of the immune response *in vivo* and *in vitro* (1, 7), we performed co-staining of MHC class I and p62, and show that p62 positive fibers were lined by sarcolemmal MHC class I in V+ and V− biopsies of IMNM patients, with MHC class I not beeing exclusively positive on p-62-positive fibers (Figure 4C). MHC class I expression was particularly elevated in V+ IMNM biopsies, (not significant as compared to V−), which is shown by semi-quantitative evaluation and exemplary immunohistochemistry (Figure 4A,B,D). However, MHC class I staining *per se* was elevated more consistently in sIBM biopsies, of note irrespective of p62-positivity or presence of vacuoles, as compared to IMNM biopsies (Figure 4D).

XBP1 and EDEM1 link ER stress to CASA-related pathways in IMNM

Since both SRP and HMGCR are localized on the ER, we studied molecules of the ER-stress response in IMNM like the ER stress response gene *XBP1*, an inducer of transcription of chaperone genes, and *EDEM1*, a molecule of which expression is induced upon upregulation of Ire1/Xbp. *EDEM1* was found at significantly higher levels in IMNM patient biopsies with vacuoles compared to sIBM (adjusted *p*-value 0.0483), while *XBP1* showed significantly different levels in both IMNM groups when compared to
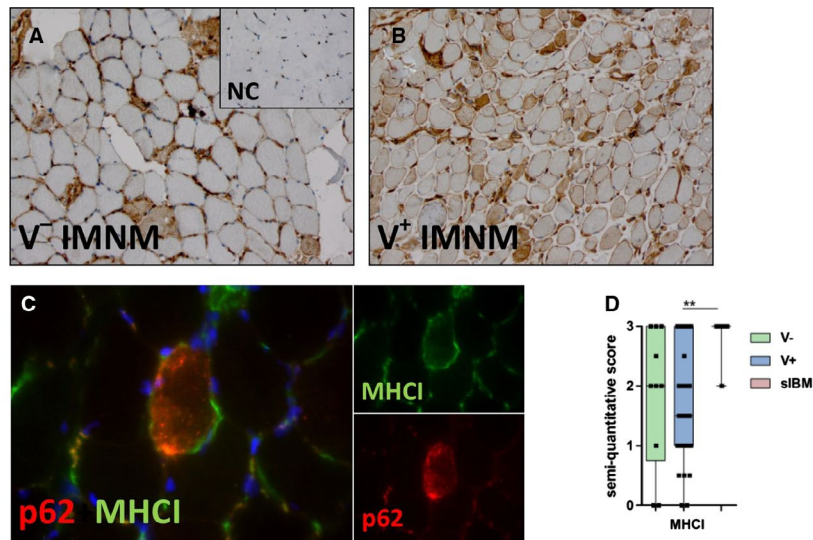
Figure 4. *Presence and relevance of MHC class I staining of myofibers in IMNM and sIBM.* Immunohistochemical MHC class I staining on the sarcolemma of myofibers is present and comparable in both groups of IMNM patients. **A**. Illustration of a moderate amount of myofibers (Score 2) with sarcolemmal and (nonspecific) sarcoplasmic MHC I deposition in a V− IMNM patient. **B**. V+ IMNM biopsy with an ample amount of sarcolemmal (and sarcoplasmic) MHC class I deposition (Score 3). In NDC muscle, no MHC class I deposition is found in myofibers with physiological MHC class I staining of capillaries (inset (NC) in A,B). **C**. Double immune fluorescence demonstrates p62 positive fibers lined by sarcolemmal MHC class I. **D**. As analyzed by the semi-quantitative scoring system, both IMNM groups show sarcolemmal and sarcoplasmic MHC class I deposition ranging from single MHC class I-positive fibers (Score 1) up to an ample amount of MHC class I staining.

sIBM (adjusted *p*-value V− vs. sIBM 0.0375 and V+ vs. sIBM 0.0004), which was due to a decreased expression of *XBP1* in sIBM. No significant increase in gene expression of *CHOP*, an ER stress induced mediator of apoptosis, was detectable in IMNM compared with NDC (data not shown). No elevated expression of these molecules was noted in sIBM (Figure 5).

DISCUSSION

In this study of skeletal muscle biopsies from 54 patients with IMNM (with 73% positive for anti-SRP or anti-HMGCR autoantibody) (3), we show clear evidence of a characteristic immunohistochemical pattern of p62 composed of a diffuse tiny dotted homogeneous pattern of the sarcoplasm in all biopsies. The staining pattern of autophagy markers in the myofibers differed from the one in sIBM and was not morphologically related to the presence of vacuoles as frequently seen in sIBM. Here, we highlight the involvement of CASA in IMNM by showing colocalization of key molecules mediating CASA like BAG3, HSP70 and HSPB5 with p62 in myofibers. In addition, we found ER stress response molecules specifically involved in the induction of chaperone-mediated protein shuttling to be increased in IMNM. Finally, we were able to link autophagy and ER stress with immune phenomena like the upregulation of MHC class I molecules in the very same fibers.

Diagnostically, the p62-staining pattern can be very useful for the correct classification of IMNM and to differentiate
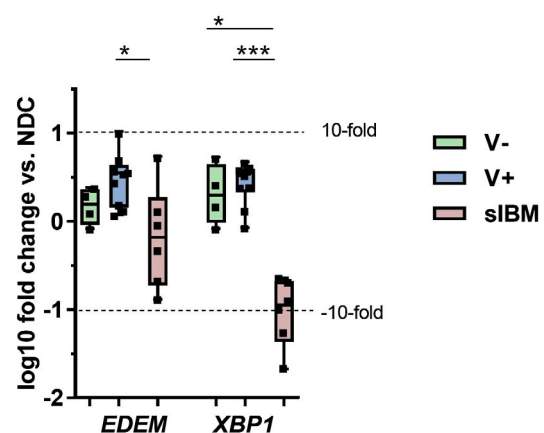

Figure 5. *Gene expression of ER-stress molecules in IMNM and sIBM.* V+ skeletal muscle biopsies show significantly increased mRNA levels of ER stress response-induced genes *EDEM1* compared with NDC, as well as sIBM patients (adjusted *p*-value 0.0483). In sIBM muscle tissues, the expression of *XBP1* was significantly reduced compared to V+ IMNM, as well as to V− (adjusted *p*-value V− vs. sIBM 0.0375 and V+ vs. sIBM 0.0004). Statistical analysis for comparison of groups was done using Kruskal-Wallis one-way ANOVA with Dunn's multiple comparison test. (*$P < 0.05$, **$P < 0.001$, ***$P < 0.0001$).

an individual IMNM biopsy from those with other possible diagnoses. Though in most cases the morphological diagnosis of IMNM is straightforward (3), it may be difficult in chronic cases or in childhood IMNM (4, 24). The intriguing fact is

that, we saw a subset of biopsies harboring vacuoles prompted us to quantify them and to study their characteristics in detail. Not only were they scarce in most cases, but they also differed from vacuoles described in sIBM (8, 10, 14, 19, 21, 33) and from the ones described in childhood or adult autophagic vacuolar myopathies (15, 27, 31, 32, 43). Vacuoles in IMNM never showed signs of the sarcolemmal lining by immunohistochemistry or electron microscopy. They also did not show any deposition of misfolded proteins or lysosomal activation by enzyme histochemistry, immunohistochemistry or electron microscopy. However, we observed nonspecific debris in small vacuoles by electron microscopy. We also observed vacuole formation particularly in muscle biopsies from patients who were biopsied late during their disease course. However, we refrained from studying this aspect since we were unable to identify the date of biopsy in all our patients. In various cell lines and in mice, a diffuse immunostaining with intense vesicular and granular character has been noted in the context of starvation (22, 30). Hence, diffuse p62 and LC3 staining implicate a rather diffuse stress response putatively involving (i) the autophagic machinery as it mediates the transfer of damaged proteins and organelles from the ER to the lysosomes and (ii) the ER, which is the main guarantor of protein homeostasis. The stressed ER, may activate the so-called UPR via the HSP70-like chaperone BiP (HSPA5) leading to the dissociation of the UPR proteins such as IRE1a mediating transcription of *Xbp1* mRNA (11). Importantly, we have measured the upregulated gene expression of these proteins in our IMNM samples, in contrast to sIBM, where the expression was reduced as compared to NDC. Interestingly, in GNE knock-in mice (M712T), mimicking the hereditary form of IBM, xbp1 was upregulated (40). Dysregulated ER stress can provoke immune dysbalance and *vice versa*, immune-inflammatory stress will itself provoke ER dysbalance (25). ER stress is probably involved in myositis pathogenesis (28) and we furthermore add specific data to this important hypothesis.

The signal recognition particle (SRP) in the cytoplasm is engaged by the signaling structure of its nascent polypeptide chain and is targeted to the SRP receptor in the ER where the protein is translocated across the ER membrane (23). This process called "co-translational translocation" involves two relevant structures, which are central players in IMNM and though the exact pathophysiological mechanisms leading to muscle damage are not fully understood, we have recently shed some light on the causative role of the autoantibody (1, 7). Anti-SRP autoantibodies are obviously targeting the protein translational structures as a potential direct stressor of the ER. Of note, also the HMGCR is located at the ER. We included a decent number of seronegative IMNM patients (some of them incompletely tested for Anti-SRP or Anti-HMGCR autoantibodies) to our study as well and the diagnosis was firmly made based on the abovementioned clinical and pathological criteria. They also exhibited the same staining pattern but we are aware that they may harbor yet undetected antibodies and
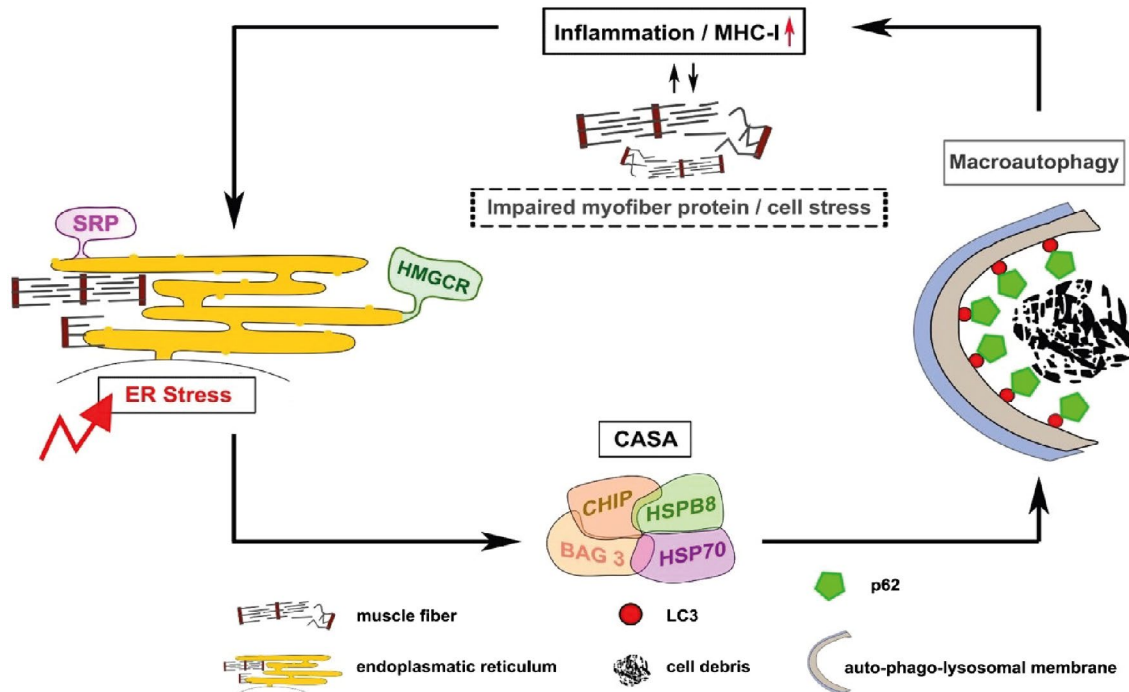
Figure 6. *Scheme of interaction between pathomechanisms involved in inflammation, autophagy and ER stress.* Antibodies against SRP are localized on the ER: since SRP is involved in proper elongation of the polypeptide chain, it is likely that defective peptides are built and ER stress is elicited. As a consequence, these defective peptides may be conducted toward and processed by CASA in terms of a myoprotective mechanism. Fibers in which this is observed are not necrotic and they upregulate MHC class I. Ultimately, this may then result in a self-perpetuating mechanism eventually leading to necrosis if these mechanisms are exhausted/decompensate.

we do not know if our hypothesis involving the ER holds true for them as well.

The autophagic-lysosomal system and the ubiquitin-proteasome machinery are of central importance for cellular protein quality control systems. Aggregated proteins can be degraded by selective macroautophagy, a multistep pathway involving HSP70, BAG3, HSPB8 as well as p62, to ensure the stability and physiological metabolism of the proteome (proteostasis) (42). We show that in IMNM, inflammatory stress conditions provoke the expression of these proteins in the same distribution pattern as described for the process of "necrosis" and "regeneration." Of note, BAG3, one of the key players of macroautophagy (29) has been shown to induce cytoplasmic puncta as sequestrated proteasomal "clients," implicated a proteasome to autophagy switch. Interestingly, cytoplasmic puncta, which have only been described *in vitro* so far, can be identified in all cases of IMNM, but not in sIBM. Conversely, in sIBM, the gene expression of *BAG3* was downregulated. This multifunctional protein, which is ubiquitously expressed in many human tissues, plays a decisive role in the development of many diseases including monogenetic myopathies (41), highlighting its key role in muscle physiology. Interestingly, the BAG3 transcript level was not altered in IMNM—but nevertheless, the protein level was significantly increased, suggesting a reduced activity of the CASA degradation pathway, which may contribute to pathology. HSP70 and HSP90 were studied in IIMs and Duchenne muscular dystrophy (DMD), but not associated with other proteins of CASA. In that study, the authors found no difference between polymyositis (PM) and sIBM and described HSP70 positivity in vacuolar fibers that strongly expressed on the rim of the vacuoles, while inflammatory cells expressed HSP90 (16).

P62 staining as a frequently used diagnostic tool in sIBM (14, 34) reveals strong immunoreactive aggregates which are rounded but sometimes linear, mainly squiggly and can be found at various degrees of intensity, strongly immunoreactive and various sizes. These authors found them in the nonvacuolated cytoplasm of approximately 80% of the vacuolated muscle fibers, and in about 20%–25% of the nonvacuolated muscle fibers. This pattern was not observed in any healthy or disease control muscle specimens (34). These authors also found increased *p62* on the mRNA level in sIBM; however, a comparison with IMNM was not performed. We also did not see this pattern in toxic myopathies and genetic myopathies with necrotic myofibers.

The ER stress response is one of the major regulatory homeostatic pathways in the skeletal muscle. Under normal, nonpathological conditions, it is activated due to, for example, exercise or dietary needs (17). However, under pathological conditions, various factors influence the pathway and its "response," such as inflammation (38). Hence, we postulate that in IMNM, the autoimmune response is significantly affecting the ER-stress response and *vice versa*. Therefore, taken together our results lead to the following pathophysiological hypothesis, for example, anti-SRP-associated IMNM (Figure 6): IMNM features autoantibodies against, for example, SRP, which is localized in the ER. Since SRP is involved in the proper elongation of polypeptide chains, it is likely that if anti-SRP autoantibodies do disturb this machinery,

defective peptides may be built and ER stress is elicited as a consequence. These defective peptides may be transferred to and processed by CASA in terms of a myoprotective mechanism, followed by autophagic processes. Fibers in which this is observed are not necrotic and they upregulate MHC class I sarcolemmal. As it was shown before, these MHC molecules can also play a role in ER stress (38). Ultimately, this may then result in a self-perpetuating mechanism eventually leading to exhaustion and necrosis.

ACKNOWLEDGMENTS

CONFLICT OF INTEREST

The authors have no conflicts of interest to declare.

DATA AVAILABILITY STATEMENT

The authors of this manuscript state that they have carefully documented data, methods and materials to conduct the research in the article. Data that are not provided in the article because of space limitations can be made available at the request of other investigators for the purpose of replicating procedures and results. To our knowledge, there are no legal or ethical reasons or any embargoes on datasets, which may restrict this data availability policy.

REFERENCES

1. Allenbach Y, Arouche-Delaperche L, Preusse C, Radbruch H, Butler-Browne G, Champtiaux N *et al* (2018) Necrosis in anti-SRP(+) and anti-HMGCR(+)myopathies: role of autoantibodies and complement. *Neurology* **90**:e507–e517.
2. Allenbach Y, Benveniste O, Goebel HH, Stenzel W (2017) Integrated classification of inflammatory myopathies. *Neuropathol Appl Neurobiol* **43**:62–81.
3. Allenbach Y, Mammen AL, Stenzel W, Benveniste O, Immune-Mediated Necrotizing Myopathies Working Group (2017) 224th ENMC International Workshop: clinico-sero-pathological classification of immune-mediated necrotizing myopathies Zandvoort, The Netherlands, 14–16 October 2016. *Neuromuscul Disord* **28**:87-99.
4. Alshehri A, Choksi R, Bucelli R, Pestronk A (2015) Myopathy with anti-HMGCR antibodies: perimysium and myofiber pathology. *Neurol Neuroimmunol Neuroinflamm* **2**:e124.
5. Arndt V, Dick N, Tawo R, Dreiseidler M, Wenzel D, Hesse M *et al* (2010) Chaperone-assisted selective autophagy is essential for muscle maintenance. *Curr Biol* **20**:143–148.
6. Arndt V, Rogon C, Hohfeld J (2007) To be, or not to be–molecular chaperones in protein degradation. *Cell Mol Life Sci* **64**:2525–2541.
7. Arouche-Delaperche L, Allenbach Y, Amelin D, Preusse C, Mouly V, Mauhin W *et al* (2017) Pathogenic role of

anti-SRP and anti-HMGCR antibodies in necrotizing myopathies: myofiber atrophy and impairment of muscle regeneration in necrotizing autoimmune myopathies. *Ann Neurol* **81**:538–548.

8. Askanas V, Engel WK, Nogalska A (2015) Sporadic inclusion-body myositis: a degenerative muscle disease associated with aging, impaired muscle protein homeostasis and abnormal mitophagy. *Biochim Biophys Acta* **1852**:633–643.

9. Bento CF, Renna M, Ghislat G, Puri C, Ashkenazi A, Vicinanza M et al (2016) Mammalian Autophagy: How Does It Work? *Annu Rev Biochem* **85**:685–713.

10. Benveniste O, Stenzel W, Hilton-Jones D, Sandri M, Boyer O, van Engelen BG (2015) Amyloid deposits and inflammatory infiltrates in sporadic inclusion body myositis: the inflammatory egg comes before the degenerative chicken. *Acta Neuropathol* **129**:611–624.

11. Bettigole SE, Glimcher LH (2015) Endoplasmic reticulum stress in immunity. *Annu Rev Immunol* **33**:107–138.

12. Bhattarai S, Ghannam K, Krause S, Benveniste O, Marg A, de Bruin G et al (2016) The immunoproteasomes are key to regulate myokines and MHC class I expression in idiopathic inflammatory myopathies. *J Autoimmun* **75**:118–129.

13. Bjorkoy G, Lamark T, Brech A, Outzen H, Perander M, Overvatn A et al (2005) p62/SQSTM1 forms protein aggregates degraded by autophagy and has a protective effect on huntingtin-induced cell death. *J Cell Biol* **171**:603–614.

14. Brady S, Squier W, Sewry C, Hanna M, Hilton-Jones D, Holton JL (2014) A retrospective cohort study identifying the principal pathological features useful in the diagnosis of inclusion body myositis. *BMJ Open* **4**:e004552.

15. Bucelli RC, Arhzaouy K, Pestronk A, Pittman SK, Rojas L, Sue CM et al (2015) SQSTM1 splice site mutation in distal myopathy with rimmed vacuoles. *Neurology* **85**:665–674.

16. De Paepe B, Creus KK, Martin JJ, Weis J, De Bleecker JL (2009) A dual role for HSP90 and HSP70 in the inflammatory myopathies: from muscle fiber protection to active invasion by macrophages. *Ann N Y Acad Sci* **1173**:463–469.

17. Deldicque L, Hespel P, Francaux F (2012) Endoplasmic Reticulum Stress in Skeletal Muscle: origin and Metabolic Consequences. *Exerc Sport Sci Rev* **40**:43–49.

18. Gamerdinger M, Carra S, Behl C (2011) Emerging roles of molecular chaperones and co-chaperones in selective autophagy: focus on BAG proteins. *J Mol Med* **89**:1175–1182.

19. Girolamo F, Lia A, Amati A, Strippoli M, Coppola C, Virgintino D et al (2013) Overexpression of autophagic proteins in the skeletal muscle of sporadic inclusion body myositis. *Neuropathol Appl Neurobiol* **39**:736–749.

20. Guttsches AK, Brady S, Krause K, Maerkens A, Uszkoreit J, Eisenacher M et al (2017) Proteomics of rimmed vacuoles define new risk allele in inclusion body myositis. *Ann Neurol* **81**:227–239.

21. Hiniker A, Daniels BH, Lee HS, Margeta M (2013) Comparative utility of LC3, p62 and TDP-43 immunohistochemistry in differentiation of inclusion body myositis from polymyositis and related inflammatory myopathies. *Acta Neuropathol Commun* **1**:29.

22. Jager S, Bucci C, Tanida I, Ueno T, Kominami E, Saftig P, Eskelinen EL (2004) Role for Rab7 in maturation of late autophagic vacuoles. *J Cell Sci* **117**:4837–4848.

23. Kang EH, Lee SJ, Ascherman DP, Lee YJ, Lee EY, Lee EB, Song YW (2016) Temporal relationship between cancer and myositis identifies two distinctive subgroups of cancers: impact on cancer risk and survival in patients with myositis. *Rheumatology* **55**:1631–1641.

24. Liang WC, Uruha A, Suzuki S, Murakami N, Takeshita E, Chen WZ et al (2017) Pediatric necrotizing myopathy associated with anti-3-hydroxy-3-methylglutaryl-coenzyme A reductase antibodies. *Rheumatology* **56**:287–293.

25. Liou HC, Boothby MR, Finn PW, Davidon R, Nabavi N, Zeleznik-Le NJ et al (1990) A new member of the leucine zipper class of proteins that binds to the HLA DR alpha promoter. *Science* **247**:1581–1584.

26. Lloyd TE, Mammen AL, Amato AA, Weiss MD, Needham M, Greenberg SA (2014) Evaluation and construction of diagnostic criteria for inclusion body myositis. *Neurology* **83**:426–433.

27. Malicdan MC, Nishino I (2012) Autophagy in lysosomal myopathies. *Brain Pathol* **22**:82–88.

28. Miller FW, Lamb JA, Schmidt J, Nagaraju K (2018) Risk factors and disease mechanisms in myositis. *Nat Rev Rheumatol* **14**:255–268.

29. Minoia M, Boncoraglio A, Vinet J, Morelli FF, Brunsting JF, Poletti A et al (2014) BAG3 induces the sequestration of proteasomal clients into cytoplasmic puncta: implications for a proteasome-to-autophagy switch. *Autophagy* **10**:1603–1621.

30. Mizushima N, Yamamoto A, Matsui M, Yoshimori T, Ohsumi Y (2004) In vivo analysis of autophagy in response to nutrient starvation using transgenic mice expressing a fluorescent autophagosome marker. *Mol Biol Cell* **15**:1101–1111.

31. Munteanu I, Ramachandran N, Ruggieri A, Awaya T, Nishino I, Minassian BA (2015) Congenital autophagic vacuolar myopathy is allelic to X-linked myopathy with excessive autophagy. *Neurology* **84**:1714–1716.

32. Nishino I, Carrillo-Carrasco N, Argov Z (2015) GNE myopathy: current update and future therapy. *J Neurol Neurosurg Psychiatry* **86**:385–392.

33. Nogalska A, D'Agostino C, Engel WK, Cacciottolo M, Asada S, Mori K, Askanas V (2015) Activation of the unfolded protein response in sporadic inclusion-body myositis but not in hereditary GNE inclusion-body myopathy. *J Neuropathol Exp Neurol* **74**:538–546.

34. Nogalska A, Terracciano C, D'Agostino C, King Engel W, Askanas V (2009) p62/SQSTM1 is overexpressed and prominently accumulated in inclusions of sporadic inclusion-body myositis muscle fibers, and can help differentiating it from polymyositis and dermatomyositis. *Acta Neuropathol* **118**:407–413.

35. Norton N, Li D, Rieder MJ, Siegfried JD, Rampersaud E, Zuchner S et al (2011) Genome-wide studies of copy number variation and exome sequencing identify rare variants in BAG3 as a cause of dilated cardiomyopathy. *Am J Hum Genet* **88**:273–282.

36. Noury JB, Maisonobe T, Richard P, Delague V, Malfatti E, Stojkovic T (2018) Rigid spine syndrome associated with sensory-motor axonal neuropathy resembling Charcot-Marie-Tooth disease is characteristic of Bcl-2-associated athanogene-3 gene mutations even without cardiac involvement. *Muscle Nerve* **57**:330–334.

37. Preusse C, Allenbach Y, Hoffmann O, Goebel HH, Pehl D, Radke J et al (2016) Differential roles of hypoxia and innate immunity in juvenile and adult dermatomyositis. *Acta Neuropathol Commun* **4**:45.

38. Rayavarapu S, Coley W, Nagaraju K (2012) Endoplasmic reticulum stress in skeletal muscle homeostasis and disease. *Curr Rheumatol Rep* **14**:238–243.

39. Rose MR (2013) 188th ENMC International Workshop: Inclusion Body Myositis, 2–4 December 2011, Naarden, The Netherlands. *Neuromuscul Disord* **23**:1044–1055.

40. Sela M (2006) Immunomodulatory vaccines against autoimmune diseases. *Rejuvenation Res* **9**:126–133.

41. Selcen D, Muntoni F, Burton BK, Pegoraro E, Sewry C, Bite AV, Engel AG (2009) Mutation in BAG3 causes severe dominant childhood muscular dystrophy. *Ann Neurol* **65**:83–89.

42. Sturner E, Behl C (2017) The role of the multifunctional BAG3 protein in cellular protein quality control and in disease. *Front Mol Neurosci* **10**:177.

43. Weihl CC, Iyadurai S, Baloh RH, Pittman SK, Schmidt RE, Lopate G *et al* (2015) Autophagic vacuolar pathology in desminopathies. *Neuromuscul Disord* **25**:199–206.

44. Weihl CC, Mammen AL (2017) Sporadic inclusion body myositis - a myodegenerative disease or an inflammatory myopathy. *Neuropathol Appl Neurobiol* **43**:82–91.

SUPPORTING INFORMATION

Additional supporting information may be found in the online version of this article at the publisher's web site:

Figure S1. Exemplary staining of LC3 (a), p62 (b) and LAMP (c) in non-disease controls. Magnification 200x.

Figure S2. p62 stains in IMNM skeletal muscle biopsies show a diffuse distribution of p62 throughout the entire sarcoplasm (a-d) with variable intensity ranging from a subtle pattern of small puncta (a) over increasing density of the puncta (b and # in d) up to a strong staining of the entire myofiber (* in d). Magnification 400x.

Figure S3. a: p62 in sIBM appear as coarse circumscribed deposits in the sarcoplasm, close to the sarcolemma or surrounding the nucleus (not visible in this exemplary picture). Mild and focal / incomplete / irregular HSP70 (b) and aB-crystallin (c) positive staining pattern of some fibers. No significant BAG3 positive fibers (d). Magnification A: 400x, B-D: 200x.